공학석사 학위논문

아민 기능화 된 규조토를 이용한 병원균 진단을 위한 단일 튜브 방법

A single-tube method for pathogen diagnostics using amine-functionalized diatomaceous earth

울 산 대 학 교 대 학 원

의 학 과

이 은 영

아민 기능화 된 규조토를 이용한

병원균 진단을 위한 단일 튜브 방법

지 도 교 수　　신　　용

이 논문을 공학석사 학위 논문으로 제출함

2018년 12월

울 산 대 학 교 대 학 원

의　　학　　과

이 은 영

이은영의 공학석사 학위논문을 인준함

심사위원 최 경 철 (인)

심사위원 주 진 명 (인)

심사위원 신 용 (인)

울 산 대 학 교 대 학 원

2018 년 12 월

ABSTRACT

Simple and efficient sample preparation is desirable for point-of-care testing of emerging diseases such as zoonoses, but current sample preparation assays are insensitive, labour-intensive and time-consuming and require multiple instruments. In this study, we developed an amine-functionalized, diatomaceous earth (DE)-based, homobifunctional imidoesters (HI) reagents assisted single-tube extraction system as a novel binding strategy to improve the solid phase extraction (SPE) method for rapid and simple purification of nucleic acid from biological samples including human cells and pathogens. A complex of amine-modified DE and HI reagents were used for nucleic acid extraction from the zoonotic pathogen, *Brucella ovis*. Using our single-tube approach, the pathogenic nucleic acid can be extracted within 20 min at a level of 1 colony formation unit (CFU). This single-tube system is based on reversible cross-linking reactions between nucleic acid and the silica matrix. The formation of robust covalent bonds protects nucleic acid, especially RNA, from both the difficulty of washing steps and isolation with ribonuclease (RNase)-rich samples leading to the extraction of higher quality nucleic acid. The performance of this approach is 10–100 times better than that of a commercial kit (10^2 to 10^3 CFU mL^{-1}) but does not require a large centrifuge. Compared to standard solid phase extraction based commercial kits, our single-tube system can be efficiently isolate pathogenic nucleic acid in human urine and serum, and the detection limit is enhanced by up to 100 times (1 CFU mL^{-1} in urine and serum). This system is fast and highly sensitive and thus represents a promising approach for sample preparation in the point-of-care testing.

Keywords: Point-of-care, Pathogen diagnosis, Reversible cross-linking reaction, Nucleic acid extraction, Homobifunctional imidoester

CONTENTS

LIST OF TABLES & FIGURES

1. INTRODUCTION

Over the past few decades, due to the increased threat of highly pathogenic infections such as, Middle east respiratory syndrome-coronavirus, Zika, H7N9 avian influenza, Ebola and common zoonotic pathogen such as, Brucellosis in both animal and human, interest has turned to the simple, trustworthy, rapid and identification of pathogen. Also, studies focused on the detection of artificially cultivated pathogens as pharma research continues to expand to meet the needs of patients worldwide.[1-8] Myriad diagnostic methods have been advanced, including conventional cultivation for microbes and improved techniques such as immunoassays and nucleic acid testing (NAT).[9-12] However, they generally involve fastidious pretreatments (e.g. high-speed sample centrifugation) that require high-cost reagents, skilled technicians, specific instruments and multiple steps. To overcome these problems related to the molecular diagnosis of pathogenic nucleic acid, a new method is needed to efficiently isolate pathogenic nucleic acid in the field to diagnose the on-site diagnosis essential for disease monitoring.[13] So new solutions that include rapid, reliable, sensitive, simple, and inexpensive can detect pathogens in various clinical environments.[14] Countless methods have been developed for nucleic acid isolation system.[15] According to the extraction phase, liquid−liquid extraction (LLE) or solid-phase extraction (SPE)[16] are generally used. Various materials are used with the SPE method, such as silica-based matrixes,[17] magnetic beads,[18] and anion-exchange membranes.[19] Among them, the silica-based SPE method is the most widely used because it can achieve nucleic acid selective precipitation on the surface of silica in the presence of chaotropic reagents.[20] However, downstream analyses such as polymerase chain reaction (PCR) are inhibited by residual chaotropic reagents.[21] Additionally, competitive absorption such as absorption of proteins onto the silica surface can reduce the SPE binding capacity.[22]

Here, we describe a simple and low-cost single-tube method for the diagnosis of zoonotic pathogen that involves on-site nucleic acid extraction. We manipulate diatomaceous

earth (DE) as a main substance for diagnostic purposes. DE is a natural bio-compatible silica and low cost used in a variety of applications such as photonics and drug delivery.[23-24] DE used in various research areas because of its large surface/volume ratio and strong adsorption capacity when combined with other materials such as nano-silicon anode and graphene.[25-29] To use DE for diagnostic purposes, pure DE was amine-functionalized by 3-aminopropyltriethoxysilane (APTES) and 3-aminopropyl(diethoxy)methylsilane (APDMS). Homobifunctional imidoesters (HI) which contain two imidoester groups at both terminals, were used in this single-tube system for nucleic acid isolation due to the reversible cross-linking reaction between nucleic acid fragments and the amine groups of amine-functionalized DE. *Brucella ovis*, one of the global zoonotic pathogens causing tremendous financial losses and high human incidence rates[30] and is used to evaluate the performance of this method. Using our single-tube approach, the pathogenic nucleic acid can be extracted within 20 min (in RNA) at a level of 1 colony formation unit (CFU) from a 1 ml sample volume in the same tube without large instruments. The performance of this approach is 10–100 times better than a commercial kit. We believe that this single-tube system can be tailored for commercial applications for not only disease diagnostics in clinical applications, but also for gene expression analysis in forensics studies. This single-tube extraction system integrated with quantitative polymerase chain reaction (qPCR) is evaluated for pathogen diagnostics. Compared with solid-phase extraction based commercialized kits, this single-tube method shows highly enhanced sensitivity with 100-fold higher sensitivity for pathogenic nucleic acid extraction, according to the cycle threshold value of qPCR and reverse transcript qPCR (RT-qPCR).

2. MATERIALS AND METHODS

2.1 Pretreatment of the extraction matrix

Diatomaceous earth (DE, calcined powder, Sigma-Aldrich) was washed with de-ionized (DI) water for 30 min with vigorous stirring. Sediment containing impurities were removed after short period of settling under gravity. Amine-functionalized DE was utilized as matrix in both the enrichment and extraction processes. Four types of silanes ((3-aminopropyl) triethoxysilane (APTES, 99%, Sigma-Aldrich), 3-aminopropyl (diethoxy)methylsilane (APDMS, 97%, Sigma-Aldrich), [3-(2-aminoethylamino) propyl] trimethoxysilane (AEAPTMS, 80%, Sigma-Aldrich) and N1-(3-trimethoxysilylpropyl) diethylenetriamine (TPDA, technical grade, Sigma-Aldrich)) were used to prepare amine-functionalized DE. Briefly, 5 mL of silane was pipetted dropwise into 100 mL 95% (v/v) ethanol solution, which was acidified with acetic acid (pH 5). 2 g of DE was then added under vigorous stirring. The reaction was maintained at room temperature (RT) for 4 h. The amine-functionalized DE was washed with ethanol and then dried under vacuum overnight. The dried amine-functionalized DE was stored at RT until further analysis.

2.2 Cell and bacteria culture

Human colon cancer cells (HCT 116) were grown at 37 °C in Dulbecco's modified Eagle's media (Life Technologies, Carlsbad, CA, U.S.A.) supplemented with 10% fetal bovine serum. pH was controlled by maintaining a 5% CO_2 atmosphere. After culturing, cell stock suspensions were counted using a cell hemocytometer, and then diluted in phosphate-buffered saline (PBS). *B. ovis* (ATCC 25840) was grown in Brucella agar (Sigma-Aldrich) containing 5% defibrinated sheep blood (MBcell, Korea) and incubated at 37 °C in an atmosphere of 5% CO_2 for 48 h. *Escherichia coli* (ATCC 25922) was inoculated in nutrient broth medium and incubated for 24 h at 37 °C under an aerobic atmosphere. *Salmonella enterica* (ATCC 14028)

was inoculated into nutrient broth medium and incubated for 24 h at 37 °C under an aerobic atmosphere. After culturing, bacterial suspensions were quantified by the agar plate method and subsequently diluted to different concentrations in PBS.

2.3 DNA extraction process

For DNA extraction from cells or bacteria, 200 μL of sample solution was added into a tube with 20 μL of proteinase K (> 600 mAU mL^{-1}, Qiagen), 150 μL of in-house lysis buffer (100 mM Tris-HCl (pH 8.0), 10 mM ethylenediaminetetraacetic acid, 1% sodium dodecyl sulfate and 10% Triton X-100) were mixed gently with a pipette and incubated at room temperature for 1 min. Then, 40 μL of 50 mg mL^{-1} DE was added, followed by 100 μL of 100 mg mL^{-1} three types of HI reagents (dimethyl suberimidate (DMS, Sigma-Aldrich), Dimethyl pimelimidate (DMP, Sigma-Aldrich), and Dimethyl adipimidate (DMA, Sigma-Aldrich) solution. After mixing, the tube was incubated in a thermal shaker at 850 rpm for 30 min at 56 °C for DNA extraction. DNA templates from lysed cells and bacteria were immobilized on amine-functionalized DE through HI cross-linking. The supernatant was removed via a short centrifugal pulse and the pellet washed twice with 200 μL of PBS. To reverse cross-linking, 100 μL of elution buffer (10 mM sodium bicarbonate, pH > 10, adjusted by NaOH) was added and incubated for 1 min at RT. After brief centrifugation, the supernatant containing the isolated DNA was move to new 1.7 mL tube and stored at −20 °C until needed. As a positive control, the same samples were subjected to nucleic acid extraction using commercial kits (QIAamp DNA Mini Kit, Qiagen) following the manufacturers' protocols.

2.4 RNA extraction process

For RNA extraction from cells or bacteria, 200 μL of sample solution was added into a tube with 20 μL of proteinase, 150 μL of in-house lysis buffer, 30 μL pf lysozyme solution (30 mg mL^{-1} in DI water, Sigma-Aldrich) and 10 μL of RNase-Free DNase solution (Qiagen)

were added separately and incubated at room temperature for 1 min. Then, 40 μL of 50 mg mL^{-1} DE was added, followed by 100 μL of 100 mg mL^{-1} HI reagents solution. After mixing, the tube was incubated in a thermal shaker at 850 rpm for 10 min at RT for RNA extraction. RNA templates from lysed cells and bacteria were immobilized on amine-functionalized DE through HI cross-linking. The supernatant was removed via a short centrifugal pulse and the pellet washed twice with 200 μL of PBS. To reverse cross-linking, 100 μL of elution buffer was added and incubated for 1 min at RT. After brief centrifugation, the supernatant containing the isolated RNA was move to new 1.7 mL tube and stored at −20 °C until needed. As a positive control, the same samples were subjected to nucleic acid extraction using commercial kits (RNeasy Mini Kit, Qiagen) following the manufacturers' protocols.

2.5 Conventional and real-time PCR

We performed PCR and qPCR to determine the quality of isolated DNA and RT-PCR and RT-qPCR to determine the quality of extracted RNA. The primers used are listed in Table 1. The PCR cycling conditions consisted of: an initial denaturation step at 95 °C for 15 min; 40 cycles at 95 °C for 30 s, 58 °C for 30 s and at 72 °C for 30 s; and a final extension step at 72 °C for 7 min. 5 μL of DNA were amplified in a total volume of 25 μL containing PCR buffer (10X, Qiagen), 2.5 mM $MgCl_2$, 0.25 mM deoxynucleotide triphosphate, 25 pM of each primer, one unit of Taq DNA polymerase (Qiagen) and deionized (DI) water. 5 μL of isolated RNA was amplified in a total volume of 25 μL containing One-step RT-PCR buffer (5X, Qiagen), 0.25 mM deoxynucleotide triphosphate, 25 pM of each primer, 1 μL of RT-PCR One-step enzyme mix (Qiagen) and DI water. The following thermal profile was used for RT-PCR: 30 min reverse transcription at 50 °C; 15 min pre-denaturation at 95 °C; 40 cycles of 30 s at 95 °C, 30 s at 58 °C, and 30 s at 72 °C; and final extension at 72 °C for 10 min. The PCR and RT-PCR products were separated on a 2% agarose gels containing ethidium bromide (EtBr) by gel electrophoresis and imaged with a Gel-Doc System (Clinx Science Instruments, Shanghai, China). The qPCR and RT-qPCR procedures were modified from the AriaMx real-

time PCR Instrument protocol (Agilent technologies). Briefly, 5 µL of isolated DNA was amplified in a total volume of 20 µL containing 2X Brilliant III SYBR Green QPCR master mix, 25 pM of each primer and DI water. An initial pre-denaturation at 95 °C for 10 min was followed by 40 cycles at 95 °C for 10 s, at 58 °C for 20 s, and at 72 °C for 20 s, and by a cooling step at 40 °C for 30 s. For RT-qPCR, 5 µL of isolated RNA was amplified in a total volume of 20 µL containing 2X Brilliant III SYBR Green QRT-PCR master mix, 25 pM of each primer, 0.2 mM of dithiothreitol, 1 µL of RT/RNase block and DI water. The following thermal profile was used for RT-qPCR: 20 min reverse transcription at 50 °C; 15 min pre-denaturation at 95 °C; 40 cycles of 10 s at 95 °C, 20 s at 58 °C, and 20 s at 72 °C; and a cooling step at 40 °C for 30 s. The SYBR Green signals of the amplified products were acquired using an AriaMx real-time PCR (Agilent Technologies, Santa, Clara, CA, USA).

Table 1. Primer sequences used in this study

Sample	Primer	sequences (5`→3`)	Tm	Product size (bp)	Annealing temp. ( )
HCT 116	18S-F	GCT TAA TTT GAC TCA ACA CGG GA	55.6	69	60
	18S-R	AGC TAT CAA TCT GTC AAT CCT CTC	54.5		
E. coli	RodA-195F	GCA AAC CAC CTT TGG TCG	56.1	195	58
	RodA-195R	CTG TGG GTG TGG ATT GAC AT	58.4		
S. enterica	Sal-275F	TAT CGC CAC GTT CGG GCA A	59.7	275	58
	Sal-275R	TCG CAC CGT CAA AGG AAC C	58.1		
B. ovis	O223F	TGG CTC GGT TGC CAA TAT CAA	57.1	223	58
	O223R	CGC GCT TGC CTT TCA GGT CTG	61.4		

3. RESULTS

3.1 Principle of the single-tube approach for pathogenic nucleic acid extraction

A schematic diagram of improved SPE method for nucleic acid extraction based on a reversible cross-linking reaction was represented in Fig. 1. Fig. 1a shows the principle of the single-tube approach involving DE for the diagnosis of zoonotic pathogens. Under optimized conditions in nucleic acid extraction, APTES and APDMS was coated on the surface of DE, which targeted primary amines in the cross-linking reaction shown in Fig. 1b. The non-chaotropic HI reagents were used as a cross-linker to stabilize extracted nucleic acid, especially RNA strands since there are abundant primary amines located on the ribonucleotides which are the fundamental components of RNA.[31-32)] Compared with single stranded RNA, DNA presents a double-stranded structure which traps deoxyribonucleotide inside and inhibits the activities.[33)] Furthermore, we used DNase I to degrade DNA in RNA extraction process. Nucleic acid from a lysed biological sample was cross-linked with APTES-DE and APDMS−DE to form a robust covalent bond in reaction buffer represented in Fig. 1b. This acts as a novel capture reagent that recognizes the amine groups on the sticky ends of nucleic acid fragments and enables positively charged amidine linkage that further enhances the isolation of negatively charged nucleic acid via the electrostatic binding of anionic nucleic acid and cationic amidine. Because this cross-linking reaction can be reversed at high pH (pH > 10),[34)] the intermediate was reversed to release nucleic acid into the elution buffer shown in Fig. 1c. Although the phosphodiester bonds in nucleic acid are not stable at high pH, considering the base catalysis only, the reaction rate coefficient (k) of nucleic acid phosphodiester degradation cannot be faster than 0.022 min^{-1}, even at pH 14.[35)] At pH 10, the k value is 10^{-5} min^{-1} under room temperature, which is stable enough for diagnostics. Especially, since our extracted RNA samples are measured immediately, the RNA degradation which is caused by pH 10 basis catalysis is negligible to the total diagnostic process.[35)] The entire process was completed within 20 min, including the operation time. Additionally,

nucleic acid extraction using the single-tube system was performed in a single tube and required only a pipette, battery-driven vortex mixer, and spin-down devices. Thus, this single-tube system has potential for a hand-held design in the future.

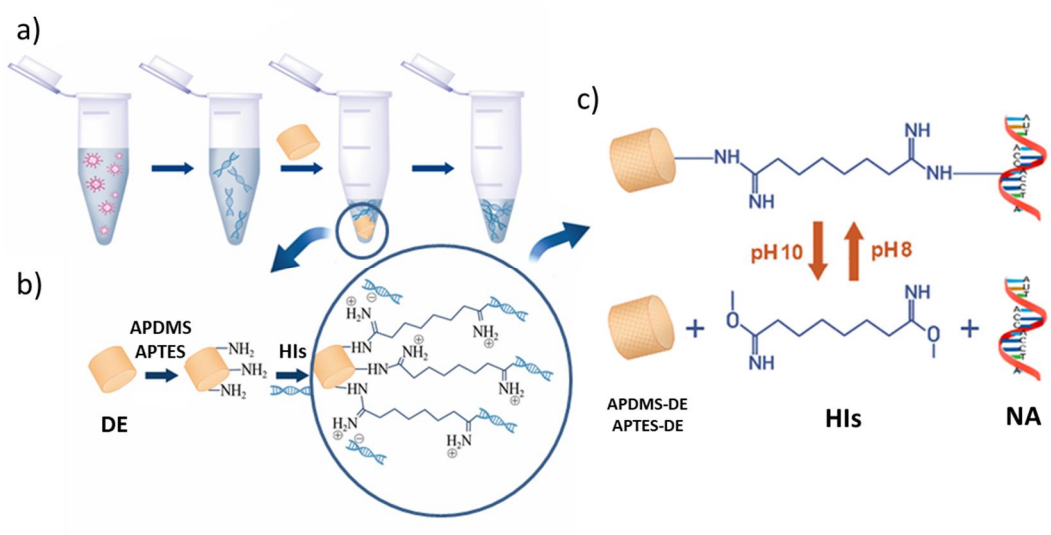

Figure 1. Schematic diagram of rapid pathogen diagnostic system using a single-tube approach via reversible cross-linking reaction. (a) Experimental nucleic acid extraction procedure. (b) Nucleic acid extraction by homobifunctional imidoester (HI) reagent-assisted APTES-DE or APDMS-DE within 30 min. (c) The assistance of the cross-linker, HI, nucleic acid from a lysed biological sample can be cross-linked with APTES-DE or APDMS−DE to form a robust covalent bond in reaction buffer (pH 8). The formed complex can be subsequently reversed to release nucleic acid in elution buffer (pH > 10). This novel system can be used for the rapid, simple diagnosis of pathogens.

3.2 Diatomaceous earth as a novel substance for extraction matrix

Purified DE mainly presents a single morphology, a micro-scale hollow in the center with numerous nano-scale pores in the wall, approximately 3 μm and 200 nm in size, respectively shown in Fig. 2. This regularly ordered nano-porous structure offers a strong physical absorption property and substantial reaction area.[36] In addition, there are abundant hydroxyl groups on its surface, which allow its chemical modification and subsequent use in biological applications, such as biotechnology and biomimetics.[24,37] Here, APTES and APDMS are selected not only for its robust coating of saline due to covalent bond formation, but also for its chemical stability compared with alkane thiols, which can be oxidized. This means that APTES-DE and APDMS-DE allows long-term storage under standard conditions. Washed and dried APTES-DE and APDMS-DE are stored in a tube at room temperature and re-dispersed in DI at 50 mg mL^{-1} for experimental use. This process is critical because it is the foundation of all subsequent experiments.

Fourier transform infrared spectroscopy (FTIR) is used to confirm the APTES functionalization process. To remove impurities and any free APTES to adequately, samples are washed three times using DI water. The FTIR spectra of plain DE and APTES-DE are presented in Fig. 2e. The absorption peak at 1072 cm^{-1} is ascribed to the asymmetric stretching vibrations of Si-O-Si, whereas the absorption peaks at 3414 and 794 cm^{-1} are attributed to Si-OH on the surface of DE. On the other hand, after the APTES modification, new absorption peaks appear at 3663, 2987, 2901, 1649, 1406, 1251, 1228 and 893 cm^{-1}. The peaks at 3663, 1649 and 893 cm^{-1} are attributed to N-H stretching, in-plane bending and out-of-plane bending vibrations, respectively. These results confirm the modification of amine groups on the surface of DE. Meanwhile, the peaks observed at 2987 and 2901 cm^{-1} can be assigned to C-H stretching vibrations and those at 1251 and 1228 cm^{-1} to C-N stretching vibrations due to amine groups directly bonded to the DE. In addition, the surface morphology of DE is changed after APTES treatment, as shown in Fig. 2d. The pore sizes of APTES-DE are significantly reduced due to the self-polymerization of APTES. These characteristics provide direct

evidence for the efficient amine functionalization of DE by APTES, which means that APTES-DE can be used in biological applications.

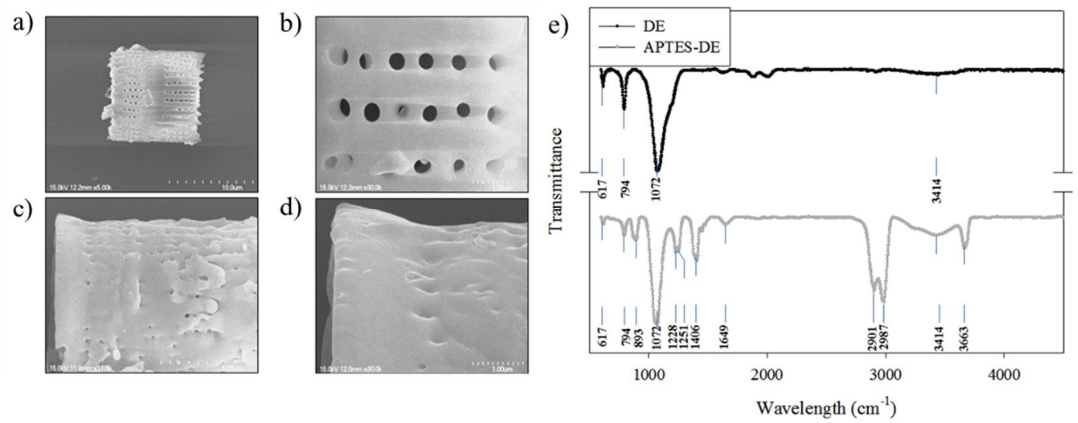

Figure 2. The SEM images and FTIR spectra of DE and APTES-DE. SEM images (a-d) and FTIR spectra (e) of DE and APTES-DE at different resolutions. a, b) Purified DE. c-d) APTES-functionalized DE. e) FTIR spectra of DE (black) and APTES-DE (grey).

3.3 Binding strategy of the single-tube system

To confirm this binding strategy, electron spectroscopy for chemical analysis (ESCA) was employed to identify the amidine bonds formed with the intermediate during the cross-linking reaction. The ESCA spectra of samples before (mixture of APDMS−DE and DMS) and after (intermediates, the remains between the washing and the elution steps) cross-linking are presented in Fig. 3. Because the amidine bond contains carbon (C) and nitrogen (N), we further analyzed the peaks belonging to C 1s of C and N 1s of N. Fig. 3a presents a wide scan of the sample that contained APDMS−DE and DMS which shows all the element peaks. As shown in Fig. 3b, according to the typical reference binding energies, three peaks of C 1s that appear at 284.5, 286.1, and 288.1 eV are attributed to the C−C and C−H bonds, the C−O bond (red) of DMS, and O−C═NH_2^+ bond (green) of DMS, respectively.[38-39] And there are two peaks of N 1s that appear in Fig. 3c, 399.3 and 401 eV, which typically belong to amine groups (−NH_2) and the O−C═NH_2^+ bond of DMS.[40] Fig. 3d presents a wide scan of the sample that came from the intermediates of the reversible cross-linking reaction. After the cross-linking reaction, because the C−O bond exhibits a stronger oxidation state than the C−N bond,[41] the binding energy of N−C═NH_2^+ (pink) should be shifted to a lower value. There are only two peaks of C 1s presented in Fig. 3e, 284.5 and 286.7 eV. Compared with Fig. 3b, the same peak of C 1s appears at 284.5 eV belonging to C−C and C−H bonds. And peaks at 286.1 and 288.1 eV disappeared because the C−O bond (286.1 eV) and the O−C═NH_2^+ (288.1 eV) were hydrolyzed and an amidine bond was formed, N−C═NH_2^+ (286.7 eV, pink).[39] In Fig. 3f, peaks of N 1s appear at 399.3 and 400.7 eV that are owed to the amine groups (−NH_2) and formed amidine bond N−C═NH_2^+, respectively. Compared with Fig. 3c, the peak that appears at 401 eV (O−C═NH_2^+) was shifted to a lower binding energy, 400.7 eV (N−C═NH_2^+), after the cross-linking reaction because of the formation of the N−C═NH_2^+ bond endowed with a weaker oxidation state than the O−C═NH_2^+ bond.[42] Furthermore, to confirm that the changes about the C 1s and N 1s peaks in Fig. 3d−f came from the RNA cross-linked with DE rather than the potential side reactions from Tris buffer or proteins (proteinase K and DNase I), we ran one more control experiment in which the sample did not contain cells while other reagents

and steps were the same, following the same protocol. At the starting point, instead of HCT 116 cells in PBS buffer, pure PBS buffer was added, following with the same protocol for lysis, incubation, and washing. The remains were dried, and the ESCA analysis was performed. As shown in Fig. 3h, C 1s peaks appeared at 284.5 eV (C−C bond), 288.1 eV (C−O bond), and 288.8 eV (COO− bond).[38] Compared with C 1s peaks (284.5 and 286.7 eV) in Fig. 3e, no N−C═NH_2^+ bond (286.7 eV) exists, but there is a C−O bond and a higher binding energy 288.8 eV (COO− bond) which belong to the hydrolysis products of DMS.[43] Likewise, in Fig. 3h, there is only one N 1s peak that appears at 399.3 eV, attributed to the amine groups, while the peak at 400.7 eV (N−C═NH_2^+ bond) is not present, which meant no cross-linking reaction occurred. Also, no peaks at 401 eV (O−C═NH_2^+ bond of DMS, Fig. 3c were observed which pointed out once again that DMS was hydrolyzed. Therefore, the changes for the C 1s and N 1s peaks in Fig. 3d−f are attributed to the formation of RNA−DE conjugations since no conjugation-specific peaks appeared in the sample prepared without cells. Above all, we confirmed the formation of an amidine bond (N−C═NH_2^+) after the cross-linking reaction, indicating that the RNA was immobilized to the surface of APDMS−DE in the presence of DMS.

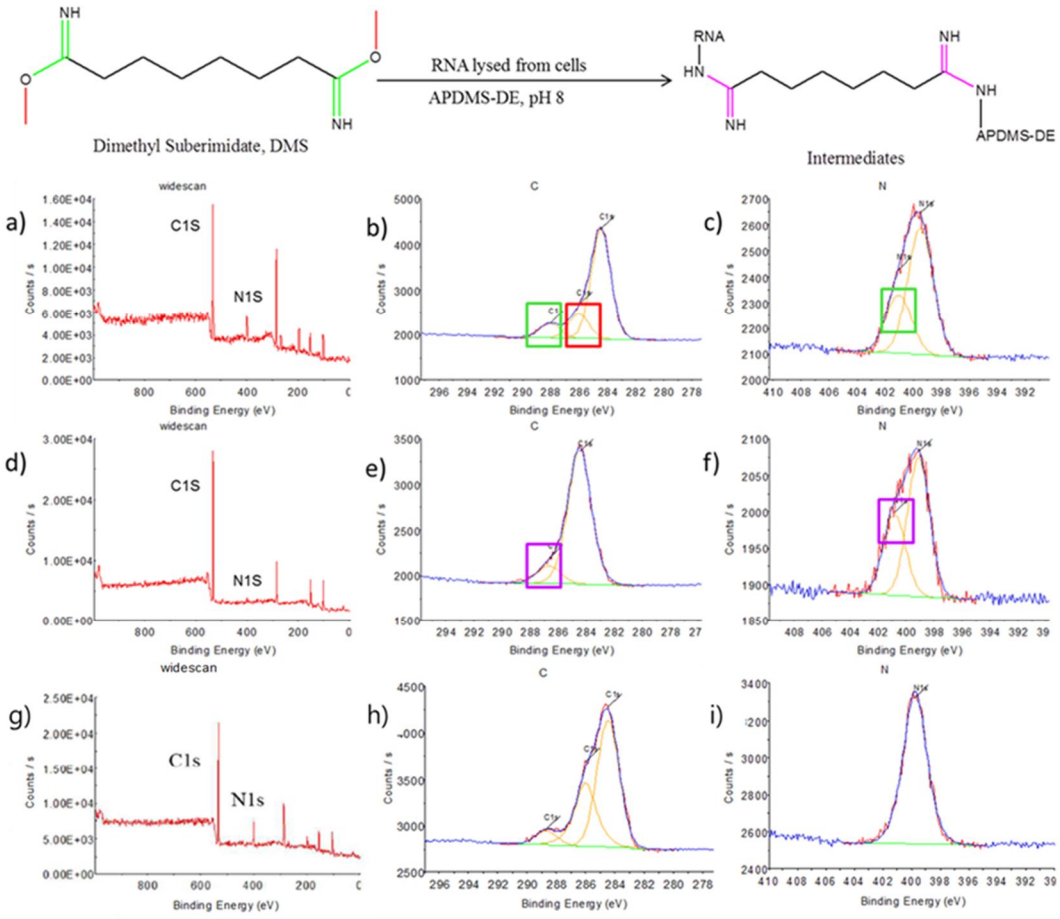

Figure 3. The ESCA spectra of samples before, after, and without cross-linking reactions. The ESCA spectra of samples before (mixture of APDMS-DE and DMS, a-c), after (intermediates, d-f) and without (no RNA existed, others are same, g-i) cross linking reactions. a), d), g) ESCA wide-scan; b), e), h) C1s of Carbon spectra; and c), f), i) N1s of Nitrogen spectra of both samples, respectively. The colored bonds in the topside chemical structures are matched with the same color box-marked ESCA peaks in panels b−e).

3.4 Characterization of DNA extraction using a complex of APTES-DE and DMS

To optimize the protocol for the single-tube system for DNA extraction purposes, we isolated high-quality DNA for subsequent qPCR analysis. During the reaction, DNA and DMS complexes bound to APTES-DE and were collected via a spin-down device. After being washed with PBS buffer, DNA was eluted via the addition of 100 μL of elution buffer and pipette mixing and spin-down. We report the DNA extraction using APTES-DE and the non-chaotropic agent DMS. DMS is selected here not only for the specific binding process, but also because the binding is reversible at high pH.[44] To determine the optimal conditions for DNA extraction, we assessed the optimal DE concentration and incubation time presented in Fig. 4a, b. Based on the qPCR results, 4 mg mL^{-1} of APTES-DE and a 20 min incubation time were the optimal conditions. Using these conditions, the performance of APTES-DE as a DNA extraction method was assessed with serially diluted samples containing from 10^0 to 10^7 CFU mL^{-1} of *B. ovis*. A linear relationship between the C_T and CFU concentration was visible in Fig. 4c, inset. This extraction process detects up to 10 CFU mL^{-1} with a high linear correlation coefficient represented in Fig. 4c ($R^2 = 0.9898$). What's more, we evaluated the performance of APTES-DE by comparing with various silica matrixes (i.e., silica gel, silica sand). The qPCR results indicated that APTES-DE was better candidate to compare with others shown in Fig. 4d. Therefore, this combination of APTES-DE and DMS can act as a novel DNA extraction tool via the assistance of a non-chaotropic agent.

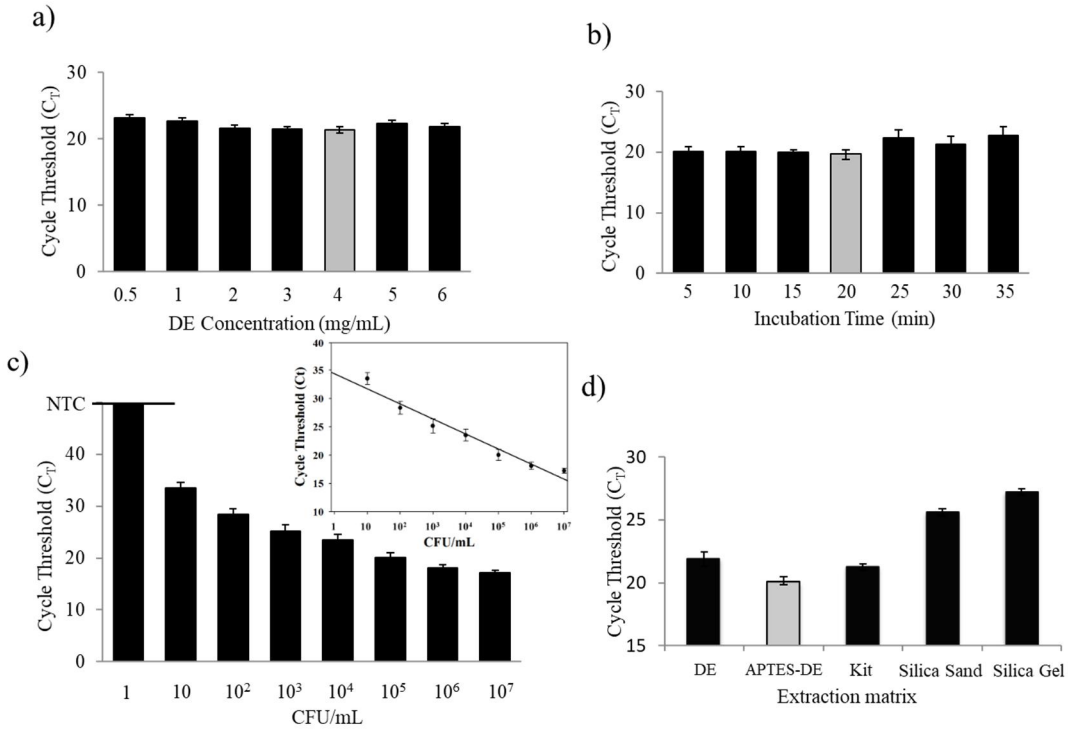

Figure 4. The characterization of the DNA extraction process using APTES-DE. The optimization of the amine-functionalized, DE-based, DMS assisted single-tube DNA extraction protocol. a–b) Optimized protocols for DNA extraction were demonstrated using qPCR with serially diluted concentrations of DE a) and at varying incubation times b). c) Performance of the DNA extraction assay using APTES-DE with a series of pathogen concentrations 10^0–10^7 CFU mL^{-1}); inset, linear relationship of the cycle threshold (C_T) as a function of the serial cell concentration. d) DNA extraction process using different silica matrix. The performance was confirmed by qPCR (*B. ovis*, 10^5 CFU mL^{-1} in PBS). Error bars indicate the standard deviation from the mean, based on at least three independent experiments. Bars extended to a negative control (NTC) line here means no amplification signals.

3.5 Optimization of RNA extraction using a complex of APDMS-DE and DMS

To optimize the protocol for the single-tube system in RNA extraction, evaluation of all components and processes in the system is required. The pretreatment extraction matrix is critical in the initial step. Typically, silane coupling agents containing organo-reactive terminals are used to functionalize inorganic matrixes. Following the DE pretreatment procedure described above, we prepared amine-functionalized DE using different silane derivatives, APTES, APDMS, AEAPTMS, and TPDA. RNA was extracted using the single-tube system and subjected to RT-qPCR analysis to compare extraction performance shown in Fig. 5a. The sample extracted by APDMS−DE showed the fastest C_T value, indicating the highest efficiency of RNA extraction.[45] Next, with respect to the efficiency of the cross-linking reaction, we tested our single-tube system using the HI reagents, DMA, DMS, and DMP. These commercially available imidoesters are commonly used in protein conjugation, but rarely in nucleic acid isolation.[44,46] The pH for the binding process was maintained around pH 8.0, because the cross-linking reaction via imidoesters presented the best reaction yield at pH 8.[47-48] Under the same experimental conditions, RNA templates from HCT 116 cells were extracted using DMA, DMS, and DMP. Based on RT-qPCR results, DMS showed the best performance in extracting RNA and thus was optimized as the cross-linker in our single-tube system shown in Fig. 5b. As the cross-linker, the amount of DMS is highly affected to the binding efficiency. Different amounts of DMS were tested and optimized based on the RT-qPCR as shown in Fig. 5c. An optimized amount was selected due to the best performance that ensured enough binding sites for RNA. Meanwhile, since DE was used as the main extraction matrix in RNA extraction step also, the performance of other silica matrixes was also investigated and presented in Fig. 5d, similar with DNA extraction shown in Fig. 4d. The C_T value of RNA sample from DE presented a much earlier cycles than others. It was attributed to the structure of DE which benefited from not only the large reaction area but also the strong absorption ability.[49] In addition, the amounts of APDMS−DE and incubation times of RNA binding also were optimized separately because these factors are responsible for the total reaction area and reaction time, respectively. As shown in Fig. 6a, more RNA was extracted

when the reaction surface area was greater. However, if the reaction surface area is too high (greater amount of APDMS−DE) in the reaction tube chamber, RNA elution can be negatively affected because more reagents (e.g. DNase I) may non-specifically adsorb to the APDMS−DE surface.[50] Thus, we selected a final concentration of 2 mg mL^{-1} APDMS−DE as reaction matrix in the single-tube system based on the RT-qPCR results shown in Fig. 6a. Using the same criterion, the optimal incubation time was found to be 10 min shown in Fig. 6b. Interestingly, even after incubation for as long as 30 min, the C_T value of single-tube system was still earlier than that of the kit, indicating that covalent bond formation prevents RNA degradation. RNA in the single-tube system was relatively stable, which is important because RNA is easily degraded in all environmental conditions.[51] We next evaluated the elution process to determine the optimum buffer pH and incubation time. As described in the binding principle, the cross-linking reaction that occurred in reaction buffer of pH 8.0 was reversed at higher pH (pH >10).[34] Therefore, the pH value of the elution buffer is critical in the single-tube system. Fig. 6c shows the differences in RT-qPCR C_T values for RNA samples eluted at high (pH > 10) or low (pH < 10) pH. The C_T value for RNA extracted in high-pH elution buffer was significantly earlier than in other buffers, indicating that cross-linked RNA is efficiently released under high-pH conditions. Although the cross-linking reaction cannot be reversed at low pH, the C_T value was highly delayed for RNA extracted in low-pH elution buffer, indicating that a small amount of RNA was released. This may be because some RNA remained physically or electrically absorbed after washing. These weak bonds were broken when the ionic concentration was changed, causing RNA to be released into low-pH elution buffer.[52] We next evaluated the effect of incubation time on RNA elution presented in Fig. 6d. We found different incubation times had negligible effects, showing a maximum of only a 2% difference. Therefore, high pH for elution buffer and 1 min for elution incubation time were selected for this single-tube method.

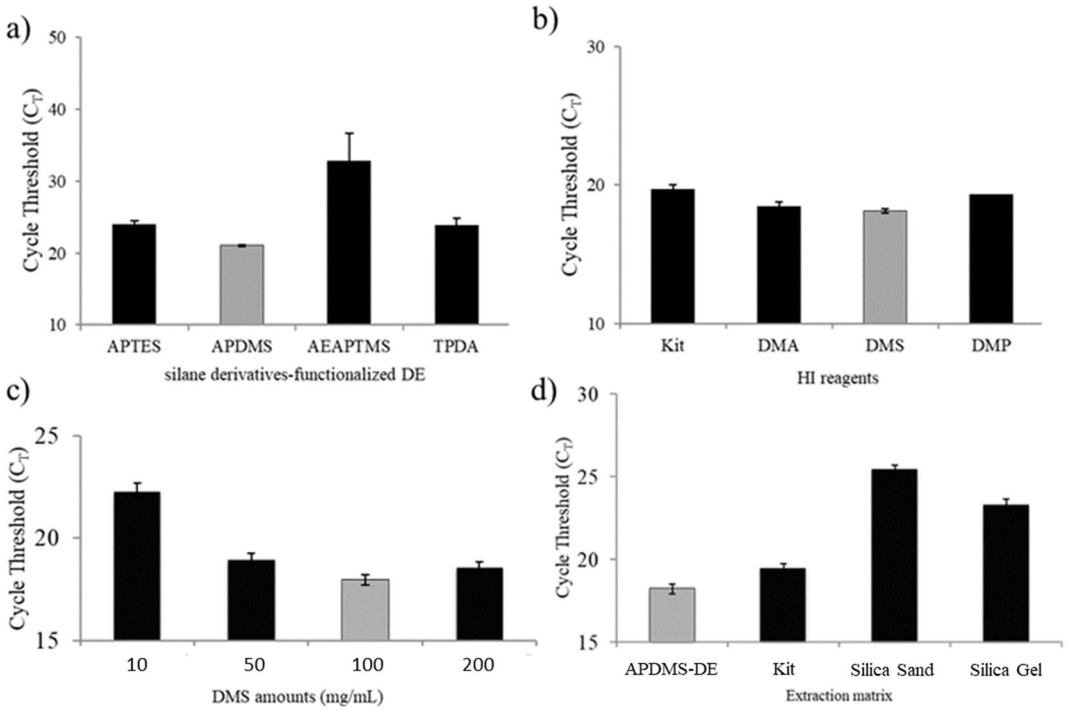

Figure 5. The optimization of the RNA extraction process using APDMS-DE with DMS. The optimization of the amine-functionalized, DE-based, DMS assisted single-tube RNA extraction protocol. The performance was evaluated by C_T value of RT-qPCR (HCT 116 cells, 10^5 cell mL^{-1}). a) C_T values of RNA extracted using different silane derivatives-functionalized DE. b) C_T values of RNA extracted using different imidoesters. c) C_T values of RNA extracted using single-tube system with different DMS amounts. d) C_T values of RNA extracted via single-tube system using different silica matrixes. The NTC showed no signal. Error bars indicate standard deviation from the mean of at least three independent experiments.

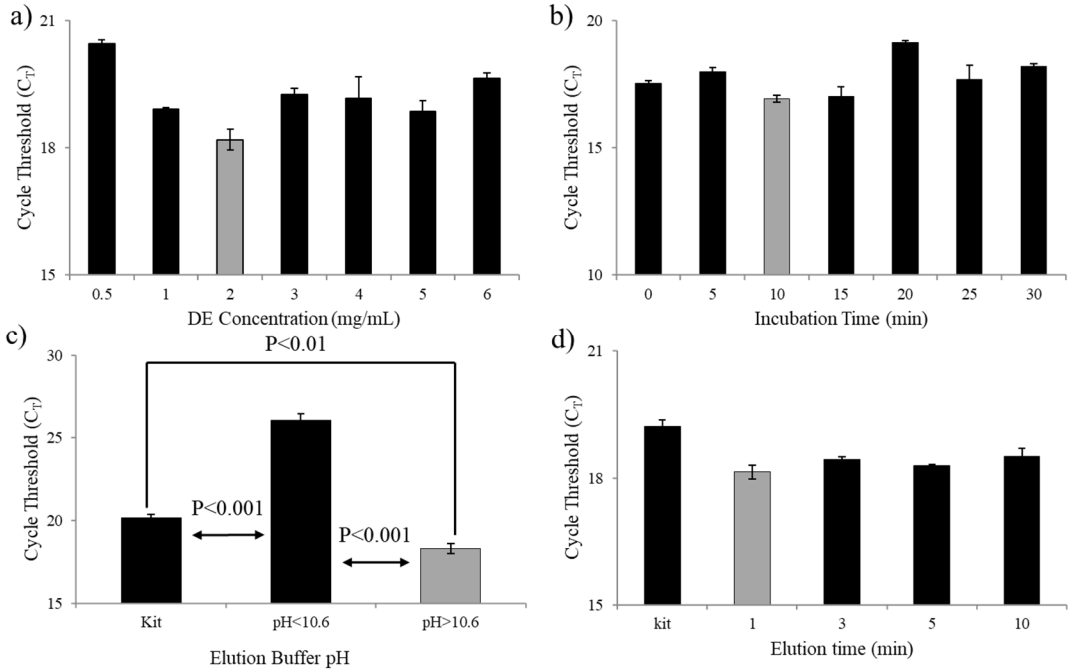

Figure 6. The optimization of single-tube system for RNA extraction based on various conditions. Optimization of amine-functionalized, DE-based, DMS assisted single-tube system for RNA extraction based on various conditions: a) C_T values of RNA extraction with different DE concentrations, b) C_T values of RNA extraction with different incubation times, c) C_T values of RNA extraction with different elution pH, d) C_T values of RNA extraction with different elution times. No C_T values were obtained for the NTC control in all the above experiments. All RNA was extracted from the same concentration of HCT 116 cell samples (10^5 cells mL^{-1}). Error bars indicate standard deviation from the mean of at least three independent experiments. The *p*-values were evaluated by Student *t* test (p-value <0.01 indicates statistically significant, and *p*-value <0.001 indicates statistically highly significant).

3.6 Validation of the Single-tube approach for DNA extraction

Because APTES-DE is used as the principal substance for DNA extraction, as detailed above, we confirmed the ability of the single-tube approach to detect pathogen in samples containing as little as 10 CFU mL^{-1}. We then examined whether this approach can be useful for the diagnosis of zoonotic pathogens in human specimens. As a systemic infection, human brucellosis appears a wide clinical spectrum while Infections of the genitourinary system are the second most common complication. It was reported that for *B. ovis* diagnosis, preputial wash samples and urine were suitable specimens.[8)] Considering of the convenience, we selected urine samples as main matrix in this study. We used spiked *B. ovis* in human urine samples at 10^2 CFU mL^{-1}. *B. ovis* was detected two cycles sooner with qPCR analysis via the single-tube approach than with the Qiagen kit presented in Fig. 7a, which means an 4- fold concentration increase.[53-54)] In addition, conventional PCR analysis also indicated that high-quality DNA was extracted via the single-tube approach (due to the presence of a clear target band) shown in Fig. 7b. We also evaluated our system using spiked *B. ovis* in animal urines (ram and dog). Similar performance was shown in Fig. 7c. The C_T value of extracted DNA by qPCR in this single-tube approach was much lower than that of the Qiagen kit presented in Fig. 7d. In addition, the performance limit was 10 times higher at 10 CFU mL^{-1} than that of the Qiagen kit (10^2 CFU mL^{-1}). To test this capability of the system, we used the samples of mixed pathogens including *B. ovis*, *S. enterica*, and *E. coli* shown in Fig. 7e. When PCR was used to amplify *S. enterica*, the target primers could be amplified the target pathogen only. Also, when PCR was used to amplify *E. coli*, the primers could be amplified the target only. Fig. 7e presented that target specific primers could only amplify the target pathogen's DNA. We further investigated this single-tube approach using low-concentration samples ranging from 10^0 to 10^3 CFU mL^{-1} of *B. ovis* in urine. Thus, we confirmed that high levels of high-quality DNA improved the detection limit of the diagnostic system.

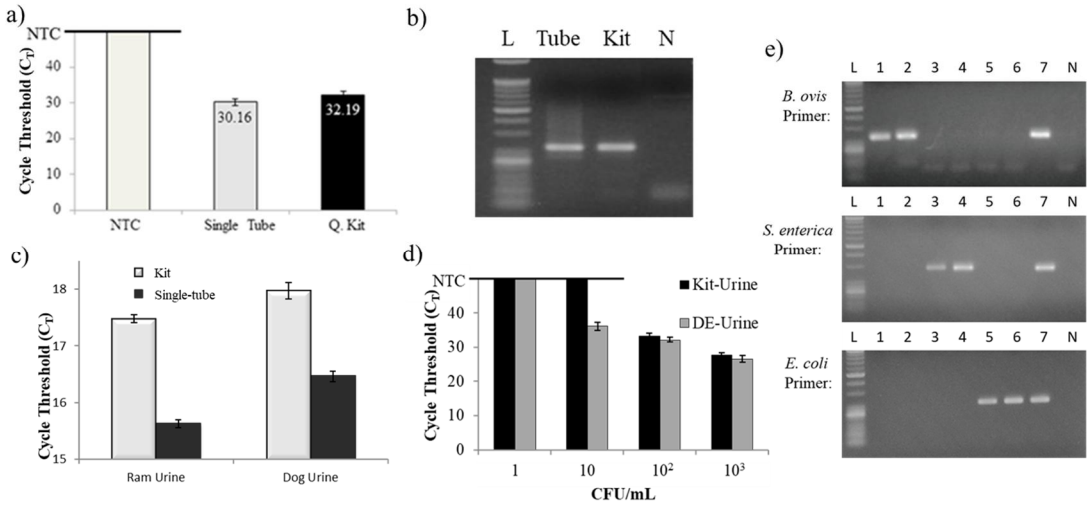

Figure 7. The performance of the single-tube approach system in urine samples. Validation of the single-tube approach using qPCR and end-point PCR methods in urine samples. a) Analysis of DNA obtained from the single-tube approach and a commercial kit using C_T values from qPCR. b) Analysis of DNA obtained from the single-tube approach and a commercial kit using an electrophoresis image after end-point PCR. c) The performance of the single-tube approach system was tested with *B. ovis* in animal urines, 10^6 CFU mL^{-1}. d) Parallel experiments comparing the performance of the commercial kit with that of the single-tube approach for analysis of *B. ovis* in urine using qPCR at low concentrations (10^0 to 10^3 CFU mL^{-1}, *B. ovis* in human urine). e) Specificity test with all three pathogen primers to a same set of pathogen DNA samples extracted by different methods: 1, *B. ovis* by kit; 2, *B. ovis* by single-tube approach; 3, *S. enterica* by kit; 4, *S. enterica* by single-tube approach; 5, *E. coli* by kit; 6, *E. coli* by single-tube approach; 7, Mixture of *B. ovis*, *S. enterica* and *E. coli*, DNA extracted by single-tube approach. All pathogens are tested with same CFU concentration, 10^4 CFU mL^{-1}. Error bars indicate the standard deviation from the mean, based on at least three independent experiments.

3.7 Evaluation of the single-tube system for RNA extraction

To evaluate the potential of using the single-tube system for RNA extraction purposes, we extracted high-quality RNA for subsequent RT-qPCR analysis. RNA samples were extracted from the same amounts of human colon cancer cell line, HCT 116 using both the single-tube method and the traditional SPE method. A commercial kit (RNeasy mini kit) was used as an SPE method in the control group. The quality of isolated RNA samples was confirmed based on the C_T value obtained by RT-qPCR analysis. Traditional SPE binding suffers from competitive absorption of various compounds (e.g. protein) and PCR inhibitors such as guanidinium or alcohols.[22] However, our proposed single-tube method overcomes these disadvantages. No chaotropic PCR inhibitors are used in the single-tube method protocol. We also detected robust covalent binding between RNA and the APDMS−DE which was more specific and allowed for more washing steps to obtain high-quality RNA. The extracted RNA was evaluated by a Nano-Drop for the quality with the ratio of absorbance at 260 and 280 nm and for the quantity with the RNA templates concentrations (ng μL^{-1}) shown in Table 2. In nucleic acid amplification-based diagnostics, the single-tube method is selective because of the use of a specific primer set targeting a relevant RNA template.[55] We tested the primers shown in Table 1. RNA templates from both the single-tube system and the kit can only be specifically amplified by the proper primers, which was confirmed by gel electrophoresis analysis of RT-PCR products. To evaluate the sensitivity of our single-tube system, parallel experiments were carried out in triplicate with serially diluted HCT 116 cells in PBS, ranging from 10^0 to 10^5 cells mL^{-1}. RNA templates of the same concentration were extracted by both single-tube method and the kit. The performance was determined by comparing the C_T values of RT-qPCR analysis. To confirm that the fluorescence signals specifically originated from the amplification of the target RNA gene template, we compared the melting temperature (Tm) of all samples. As shown in Fig. 8a-b, all amplified RNA samples showed the same Tm value, indicating that there was only one amplified product.[54] No signal appeared in the NTC. What's more, considering the potential DNA contamination, the No RT control was performed to the RT reactions as shown in Fig. 8c-d. At high sample concentration, there was a signal that came

from the No RT control. However, the C_T value of RT (18) was 15 cycles earlier than that of the No RT (33), which meant the No RT control sample corresponded to approximately 3000-fold less target templates (assuming the amplification efficiency is 100%, and then 1 C_T is approximately equal to 2-fold concentration differences of target templates).[56] At low concentration, there was no detectable signal appearing in the No RT control. Thereby, the DNA contamination was negligible since only 0.033% (1/3000) of the amplification signal for the RT process was contributed to the DNA contamination. Thus, the RT-qPCR results were specifically amplified from the targeted HCT 116 RNA template. In addition, as shown in Fig. 8a, RNA extracted by single-tube method can be successfully recovered at very low concentrations of 10^0 cells mL^{-1} (less than 10 cells), while the detection limit of the kit was 10^3 cells mL^{-1}. The sensitivity of our improved single-tube system was 1000-fold higher than that of a standard SPE-based kit. Afterward, we evaluated the binding capacity of the single-tube system. The nano-porous DE, which has a very large reaction surface (200 m^2 g^{-1}),[49] was used as an extraction matrix in our single-tube system. This novel matrix ensures a relatively high binding capacity. As mentioned in the Experimental Section, various amounts of purified RNA samples were loaded to the single-tube system and recovered via the extraction protocol. The turning point, noted the binding capacity, was confirmed when the recovered RNA amount was no longer increased under an increased amount of loaded RNA shown in Fig. 9a (1352 ng). Since the DMS hydrolysis generated a milk-like solution,[43] it is impossible to detect the unloaded RNA samples that remained in the reaction buffer that contains excessive cross-linker DMS. We evaluated the reaction yield (RY) for the total reversible cross-linking reaction including both cross-linked and reversed reactions via the ratio of total recovered RNA amount to the total loaded RNA amount shown in Fig. 9a. The RY (92.2%) was calculated only from the average RY of sufficient reactions, which was more than twice that to previously reported for 40% extraction efficiency obtained on silica presented in reactions 3−5 in Fig. 9a.[50] Furthermore, the binding capacity of this system should be qualified for the crude biological samples and HCT 116 cells (10^6, 10^7, and 10^8 cells mL^{-1}) that were incubated with the optimized single-tube system to illustrate this point. The prepared RNA samples were

subjected to RT-qPCR shown in Fig. 9b. The C_T value from the 10^7 cells mL^{-1} sample was approximately 3.2 cycles earlier than that of the 10^6 cells mL^{-1} sample, indicating a 9.2-fold higher concentration, which is similar to the predicted result (10 times).[57] However, the C_T value was not clearly decreased for the 10^8 cells mL^{-1} sample, indicating that this single-tube system is limited for high cell concentrations (up to 10^7 cells mL^{-1}).

Table 2. RNA quality test via Nanodrop

	Kit		**Single-tube**	
	High (10^6)	Low (10^3)	High (10^6)	Low (10^3)
Quantity (ng μL^{-1})	12.1±0.71	5.2±0.67	14.7±0.67	6.5±1.1
Purity (A260/A280)	1.96±0.12	1.85±0.11	1.88±0.21	1.81±0.14

Extracted RNA samples were compared with different extraction methods, both the kit extraction and single-tube system extraction, using same HCT 116 samples at 10^6 and 10^3 cells mL^{-1}, respectively.

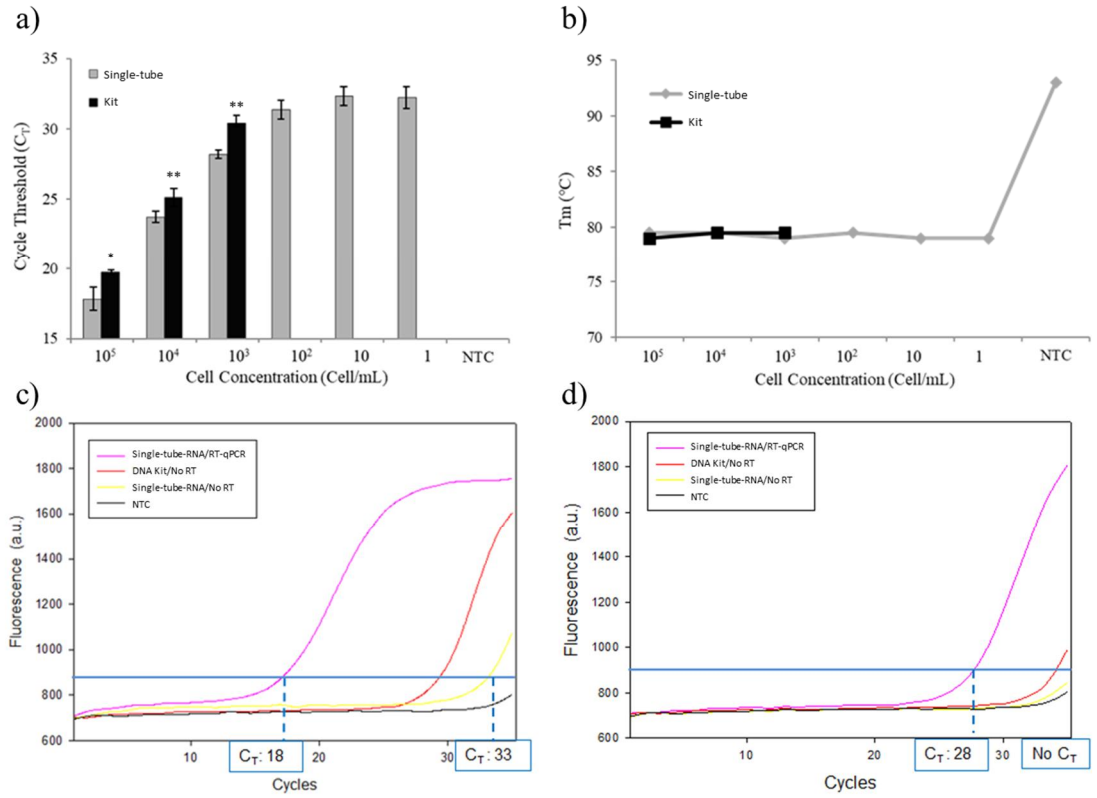

Figure 8. The performance of the single-tube system-based RNA extraction from crude biological samples. (a) C_T values of RNA extracted from serial cell concentrations of HCT 116 cells via both the amine-functionalized, DE-based, DMS assisted single-tube system (grey) and traditional SPE approach using a commercial kit (black). (b) Tm values of extracted RNA performed with RT-qPCR and DNA background evaluation of extracted RNA via the single-tube system. The same RNA sample was subjected to the RT-qPCR with both RT positive and No-RT negative controls. (c) C_T values of extracted RNA samples at high concentration (HCT 116, 10^5 cells mL^{-1}). (d) C_T values of extracted RNA samples at low concentration (HCT 116, 10^3 cells mL^{-1}). The blank of the NTC indicates that there is no signal observed from NTC. Error bars indicate the standard deviation from the mean, based on at least three independent experiments. The *p*-values were evaluated by Student *t* test (comparing both Single-tube and the Kit with same concentration samples, * *p*-value<0.05, ** *p*-value <0.01; *p*-value <0.05 indicates statistically significant, and *p*-value <0.01 indicates statistically significant).

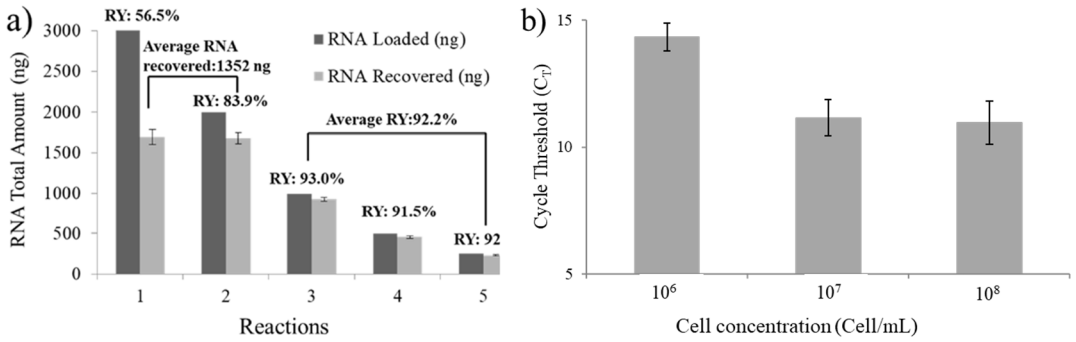

Figure 9. Binding capacity study. a) Binding capacity of purified RNA on single-tube system (1352 ng) and the total reversible crosslinking reaction yield (RY, 92.2%) of RNA isolation via single-tube system. RNA was loaded with different amounts: 1, 3000 ng; 2, 1500 ng; 3, 1000 ng; 4, 500 ng; 5, 250 ng. b) C_T values of RNA extracted by single-tube system from high-concentration HCT 116 cell samples (10^6 – 10^8 cells mL^{-1}). Error bars indicate standard deviation from the mean of at least three independent experiments.

3.8 Application of the single-tube system for diagnostics

As described above, the reversible cross-linking-based single-tube system can successfully extract nucleic acid from various biological samples. The optimized protocol was compared with a traditional SPE approach, which showed that the single-tube system may be useful for nucleic acid-based diagnostics. Human brucellosis, which is endemic in many countries and regions, is among the major zoonotic diseases worldwide.[58] We used our single-tube system to extract RNA from *B. ovis*. As shown in Fig. 10a, an ultralow *B. ovis* concentration of 10^0 CFU mL^{-1} was detected using the single-tube system, which is 100-fold higher than the performance of the SPE-based kit. The relationship between C_T values of RNA extracted by single-tube system and pathogen cell concentration presented a highly linear correlation ($R^2 = 0.979$). Fluorescence signals were confirmed to be specific based on the Tm and NTC shown in Fig. 10b. Additionally, RNA extracted from a 10^5 CFU mL^{-1} *B. ovis* sample from urine was further evaluated using the single-tube system to determine the clinical relevance of our method. Because *B. ovis* is a zoonotic pathogen, we spiked the same concentration of *B. ovis* into both human urine and ram urine samples. Although the overall C_T value of *B. ovis* in urine was delayed compared to that in PBS, the quality of RNA extracted using the single-tube system showed an earlier C_T result compared to RNA extracted using the kit shown in Fig. 10c. We also tested our single-tube system with relatively large sample volumes to increase the detection limit by loading more samples. The RT-qPCR results showed that more RNA was extracted from a large-volume (1 mL) sample by the single-tube system than by using other systems presented in Fig. 10d. The C_T value for RNA from the 1 mL sample was approximately 2 cycles earlier than that of the 200 μL sample, indicating that the amount of extracted RNA was clearly increased when the sample volume was larger. For RNA extracted using the single-tube system, although the protocol was optimized for 200 μL samples, larger volumes can also be used. Therefore, our proposed single-tube system is useful for nucleic acid extraction and detection of pathogens based on nucleic acid amplification by RT-qPCR.

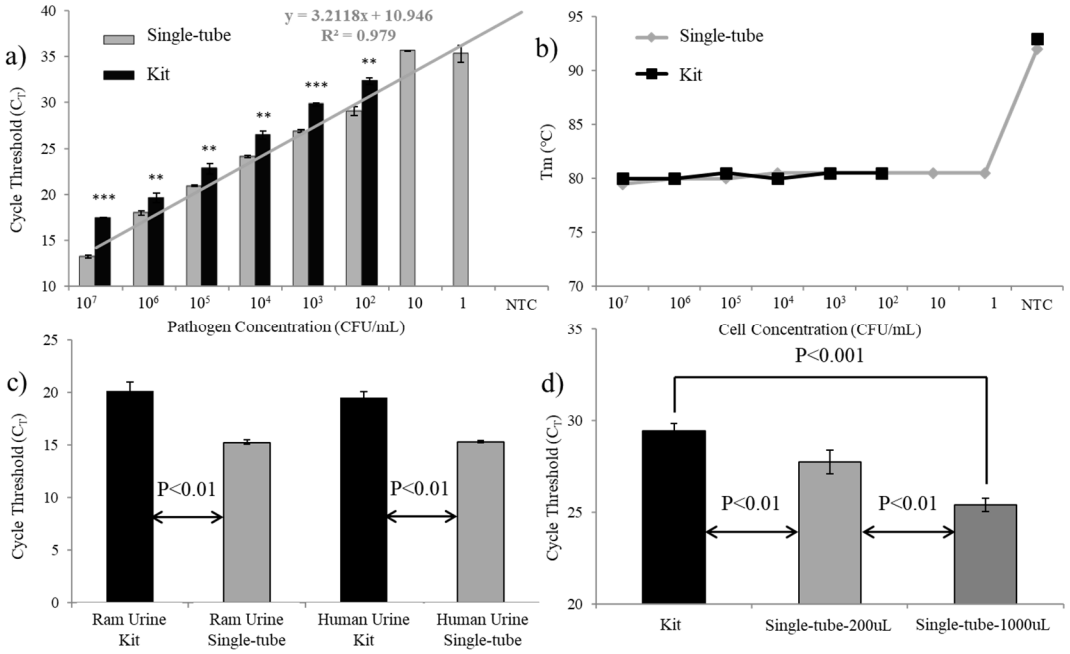

Figure 10. Performance of amine-functionalized, DE-based, DMS assisted single-tube system-based RNA extraction from pathogenic *B. ovis* samples. a) C_T values of RNA extracted from serial cell concentrations of *B. ovis* in PBS buffer via both single-tube system (grey) and traditional SPE approach using commercial kit (black). A linear relationship between C_T value of RNA extracted by single-tube and cell concentration is presented (R^2=0.979). b) Tm values of extracted RNA performed with RT-qPCR. c) C_T values of RNA extracted by both singe-tube and kit for *B. ovis* samples in urines at a concentration of 10^7 CFU mL^{-1}. d) Relatively large sample volume test of single-tube system for RNA extraction using HCT 116 cell at a concentration of 10^3 Cell mL^{-1}. The blank of NTC indicates that there is no signal observed from NTC. Error bars indicate the standard deviation from the mean, based on at least three independent experiments. The *p*-values were evaluated by Student *t* test (comparing both Single-tube and the Kit with same concentration samples, ** *p*-value<0.01, *** *p*-value <0.001; *p*-value <0.01 indicates statistically significant, and *p*-value <0.001 indicates statistically highly significant).

4. DISUCUSSION

Although numerous technological advances in the field of disease diagnostics in a few decades, many scientists, engineers and clinicians desire more appropriate technology for clinical settings. Importantly, detection sensitivity in clinical applications can be improved when high levels of high-quality nucleic acids. Thus, the new technology would need to encompass the following features: (I) nucleic acid extraction from pathogens without inhibitor in downstream analysis, (II) flexible integration with the detection system for POCT, and (III) rapid and sensitive diagnosis step. To achieve these goals, we developed a reversible cross-linking-reaction-based single-tube method for rapid and simple purification of nucleic acid from biological samples. Amine−functionalized DE was employed as a novel extraction matrix because of its very large reaction area. Nucleic acid from lysed bacteria can be linked onto the surface of amine-functionalized DE using the homobifunctional cross-linker DMS without using chaotropic reagents. The amidine bonds formed between nucleic acid and amine−functionalized DE were reversed at high pH (pH> 10), and nucleic acid was released in the elution buffer. Although silica matrixes, including DE, are widely used in SPE-based nucleic acid extraction, in this study we developed a new binding strategy to improve traditional SPE-based nucleic acid extraction by targeting the formation of reversible covalent bonds between nucleic acid and amine-functionalized DE. Nucleic acid isolated from pathogen by amine−functionalized DE were evaluated by downstream analysis (PCR). The detection limit of the improved method showed a high sensitivity when 10^0 CFU mL^{-1} was evaluated and was 100-fold higher compared to the traditional SPE method (Qiagen kit). The relevant issues have been innovatively addressed. Nucleic acid was extracted from the pathogen in the same tube without the need for large instruments. Our method involves the use of a single tube and a battery-driven spin-down device and is thus a promising candidate for point-of-care diagnosis. We envision that this combination system will be useful for not only other emerging diseases in both humans and animals but also be tailored for commercial applications for

nucleic acid expression analysis in forensics studies.

5. REFERENCES

1. Ai JW, Zhang Y, Zhang W. Zika virus outbreak: “a perfect storm.”. Emerg Microbes Infect. 2016;5:e21.

2. Baker WS, Gray GC. A review of published reports regarding zoonotic pathogen infection in veterinarians. J Am Vet Med Assoc. 2009;234:1271–8.

3. Carroll MW, Matthews DA, Hiscox JA, Elmore MJ, Pollakis G, Rambaut A, et al. Temporal and spatial analysis of the 2014-2015 Ebola virus outbreak in West Africa. Nature. 2015;524:97–101.

4. Durai P, Batool M, Shah M, Choi S. Middle East respiratory syndrome coronavirus: transmission, virology and therapeutic targeting to aid in outbreak control. Exp Mol Med. 2015;47:e181.

5. Kang DH, Kim YJ, Kim SH, Sun BJ, Kim DH, Yun SC, et al. Early surgery versus conventional treatment for infective endocarditis. N Engl J Med. 2012;366:2466–73.

6. Mäkelä MJ, Puhakka T, Ruuskanen O, Leinonen M, Saikku P, Kimpimäki M, et al. Viruses and bacteria in the etiology of the common cold. J Clin Microbiol. 1998;36:539–42.

7. Nilsson KG, Mandenius CF. A carbohydrate biosensor surface for the detection of uropathogenic bacteria. Nat Biotech. 1994;12:1376–8.

8. Xavier MN, Silva TM, Costa ÉA, Paixão TA, Moustacas VS, Carvalho CA, et al. Development and evaluation of a species-specific PCR assay for the detection of Brucella ovis infection in rams. Vet Microbiol. 2010;145:158–64.

9. Boehme CC, Nabeta P, Hillemann D, Nicol MP, Shenai S, Krapp F, et al. Rapid molecular detection of tuberculosis and rifampin resistance. N Engl J Med. 2010;363:1005–15.

10. Islam FS, Gault AG, Boothman C, Polya DA, M Charnock JM, Chatterjee D, et al. Role of metal-reducing bacteria in arsenic release from Bengal delta sediments. Nature. 2004;430:68–71.

11. Kinjo Y, Wu D, Kim G, Xing GW, Poles MA, Ho DD, et al. Recognition of bacterial glycosphingolipids by natural killer T cells. Nature. 2005;434:520–5.

12. Silk TM, Donnelly CW. Increased detection of acid-injured Escherichia coli O157:H7 in autoclaved apple cider by using nonselective repair on Trypticase soy agar. J Food Prot. 1997;60:1483–6.

13. Ivnitski D, Abdel-Hamid I, Atanasov P, Wilkins E. Biosensors for detection of pathogenic bacteria. Biosens Bioelectron. 1999;14:599–624.

14. Daar AS, Thorsteinsdóttir H, Martin DK, Smith AC, Nast S, Singer PA. Top ten biotechnologies for improving health in developing countries. Nat Genet. 2002;32:229–32.

15. Tan SC, Yiap BC. DNA, RNA, and protein extraction: the past and the present. J Biomed Biotechnol. 2009;2009:574398.

16. Arthur CL, Pawliszyn J. Solid phase microextraction with thermal desorption using fused silica optical fibers. Anal Chem. 1990;62:2145−8.

17. Tian H, Hühmer AF, Landers JP. Evaluation of silica resins for direct and efficient extraction of DNA from complex biological matrices in a miniaturized format. Anal Biochem. 2000;283:175−91.

18. Hultman T, Ståhl S, Hornes E, Uhlén M. Direct solid phase sequencing of genomic and plasmid DNA using magnetic beads as solid support. Nucleic Acids Res. 1989;17:4937−46.

19. Chang CS, Ni HS, Suen SY, Tseng WC, Chiu HC, Chou CP. Preparation of inorganic–organic anion-exchange membranes and their application in plasmid DNA and RNA

separation. J Membr Sci. 2008;311:336−48.

20. Price CW, Leslie DC, Landers JP. Nucleic acid extraction techniques and application to the microchip. Lab Chip. 2009;9:2484−94.

21. Monteiro L, Bonnemaison D, Vekris A, Petry KG, Bonnet J, Vidal R, et al. Complex polysaccharides as PCR inhibitors in feces: Helicobacter pylori model. J Clin Microbiol. 1997;35:995−8.

22. Rogacs A, Qu Y, Santiago JG. Bacterial RNA Extraction and Purification from Whole Human Blood Using Isotachophoresis. Anal Chem. 2012;84:5858−63.

23. Ehrlich H, Demadis KD, Pokrovsky OS, Koutsoukos PG. Modern Views on Desilicification: Biosilica and Abiotic Silica Dissolution in Natural and Artificial Environments. Chem Rev. 2010;110:4656–89.

24. Rosi NL, Thaxton CS, Mirkin CA. Control of nanoparticle assembly by using DNA-modified diatom templates. Angew Chem Int Ed Engl. 2004;116:5616–9.

25. Campbell B, Ionescu R, Tolchin M, Ahmed K, Favors Z, Bozhilov KN, et al. Carbon-Coated, Diatomite-Derived Nanosilicon as a High Rate Capable Li-ion Battery Anode. Sci Rep. 2016;6:33050.

26. Chen K, Li C, Shi L, Gao T, Song X, Bachmatiuk A, et al. Growing three-dimensional biomorphic graphene powders using naturally abundant diatomite templates towards high solution processability. Nat Comm. 2016;7:13440.

27. Losic D, Mitchell JG, Voelcker NH. Diatomaceous Lessons in Nanotechnology and Advanced Materials. Adv Mat. 2009;21:2947–58.

28. Melzak KA, Sherwood CS, Turner RF, Haynes CA. Driving Forces for DNA Adsorption to Silica in Perchlorate Solutions. J Colloid Interface Sci. 1996;181:635–44.

29. Qian T, Li J, Deng Y. Pore structure modified diatomite-supported PEG composites

for thermal energy storage. Sci Rep. 2016;6:32392.

30. Boschiroli ML, Foulongne V, O'Callaghan D. Brucellosis: a worldwide zoonosis. Curr Opin Microb. 2001;4:58–64.

31. Sengupta RN, Van Schie SN, Giambasu G, Dai Q, Yesselman JD, York D, et al. An active site rearrangement within the Tetrahymena group I ribozyme releases nonproductive interactions and allows formation of catalytic interactions. RNA. 2016;22:32–48.

32. Nissen P, Hansen J, Ban N, Moore PB, Steitz TA. The structural basis of ribosome activity in peptide bond synthesis. Science. 2000;289:920−30.

33. Davis IW, Leaver-Fay A, Chen VB, Block JN, Kapral GJ, Wang X, et al. MolProbity: all-atom contacts and structure validation for proteins and nucleic acids. Nucleic Acids Res. 2007;35:375−83.

34. Hermanson GT. Bioconjugate Techniques. 3rd ed. San Diego(CA): Academic Press; 2013.

35. Li Y, Breaker RR. Kinetics of RNA Degradation by Specific Base Catalysis of Transesterification Involving the 2‘-Hydroxyl Group. J Am Chem Soc. 1999;121:5364−72.

36. Yang W, Lopez PJ, Rosengarten G. Diatoms: self assembled silica nanostructures, and templates for bio/chemical sensors and biomimetic membranes. Analyst. 2011;136:42–53.

37. Townley HE, Parker AR, White-Cooper H. Exploitation of Diatom Frustules for Nanotechnology: Tethering Active Biomolecules. Adv Funct Mater. 2008;18:369–74.

38. Okpalugo TI, Papakonstantinou P, Murphy H, McLaughlin J, Brown NM. High resolution XPS characterization of chemical functionalised MWCNTs and SWCNTs. Carbon. 2005;43:153−61.

39. Bai H, Xu Y, Zhao L, Li C, Shi G. Non-covalent functionalization of graphene sheets by sulfonated polyaniline. Chem Commun. 2009;1667−9.

40. Jin YG, Qiao SZ, da Costa JC, Wood BJ, Ladewig BP, Lu GQ. Hydrolytically Stable Phosphorylated Hybrid Silicas for Proton Conduction. Adv Funct Mater. 2007;17:3304−11.

41. Huang YL, Tien HW, Ma CM, Yang SY, Wu SY, Liu HY, et al. Effect of extended polymer chains on properties of transparent graphene nanosheets conductive film. J Mater Chem. 2011;21:18236−41.

42. Lai L, Potts JR, Zhan D, Wang L, Poh CK, Tang C, et al. Exploration of the active center structure of nitrogen-doped graphene-based catalysts for oxygen reduction reaction. Energy Environ Sci. 2012;5:7936−42.

43. Pan DW, Davis ME. Cationic mucic acid polymer-based siRNA delivery systems. Bioconjugate Chem. 2015;26:1791-803.

44. Shin Y, Perera AP, Tang WY, Fu DL, Liu Q, Sheng JK, et al. A rapid amplification/detection assay for analysis of Mycobacterium tuberculosis using an isothermal and silicon bio-photonic sensor complex. Biosens Bioelectron. 2015;68:390–6.

45. Gibson UE, Heid CA, Williams PM. A novel method for real time quantitative RT-PCR. Genome Res. 1996;6:995−1001.

46. Liu FT, Zinnecker M, Hamaoka T, Katz DH. New procedures for preparation and isolation of conjugates of proteins and a synthetic copolymer of D-amino acids and immunochemical characterization of such conjugates. Biochemistry. 1979;18:690−7.

47. Hand ES, Jencks WP. Mechanism of the Reaction of Imido Esters with Amines. J Am Chem Soc. 1962;84:3505−14.

48. Kazan D, Ertan H, Erarslan A. Stabilization of penicillin G acylase against pH by

chemical cross-linking. Process Biochem. 1996;31:135−40.

49. Napierska D, Thomassen LC, Lison D, Martens JA, Hoet PH. The nanosilica hazard: another variable entity. Part Fibre Toxicol. 2010;7:39.

50. Hagan KA, Meier WL, Ferrance JP, Landers JP. Chitosan-Coated Silica as a Solid Phase for RNA Purification in a Microfluidic Device. Anal Chem. 2009;81:5249−56.

51. Sampaio-Silva F, Magalhães T, Carvalho F, Dinis-Oliveira RJ, Silvestre R. Profiling of RNA degradation for estimation of post mortem [corrected] interval. PLoS One. 2013;8:e56507.

52. Steinbacher JL, Landry CC. Adsorption and release of siRNA from porous silica. Langmuir. 2014;30:4396−405.

53. He L, Chinnery PF, Durham SE, Blakely EL, Wardell TM, Borthwick GM, et al. Detection and quantification of mitochondrial DNA deletions in individual cells by real-time PCR. Nucleic Acids Res. 2002;30(14):e68.

54. Heid CA, Stevens J, Livak KJ, Williams PM. Real time quantitative PCR. Genome Res. 1996;6:986–94.

55. Lazcka O, Del Campo FJ, Muñoz FX. Pathogen detection: a perspective of traditional methods and biosensors. Biosens Bioelectron. 2007;22:1205−17.

56. Rychlik W, Spencer WJ, Rhoads RE. Optimization of the annealing temperature for DNA amplification in vitro. Nucleic Acids Res. 1990;18:6409−12.

57. Fleige S, Pfaffl MW. RNA integrity and the effect on the real-time qRT-PCR performance. Mol Aspects Med. 2006;27:126–39.

58. Pappas G, Papadimitriou P, Akritidis N, Christou L, Tsianos EV. The new global map of human brucellosis. Lancet Infect Dis. 2006;6:91−9.

6. 국문요약

동물원성 감염병과 같은 신생 질병에 대한 현장 진단 검사에는 간단하고 효율적인 시료 준비가 바람직하지만, 현재 시료 준비 및 분석은 민감하지 않고, 노동 집약적이며, 시간 소모적이며, 여러 장비가 필요하다. 본 연구에서는 고체상 추출 (solid phase extraction, SPE) 방법을 개선하기 위한 새로운 결합 방법으로 아민 기능화 된 규조토와 동형2기능성 이미도에스터 (Homobifunctional imidoester, HI)를 사용하여 신속하고 간단하게 병원균 및 세포를 포함하는 생물학적 시료에서 핵산을 추출하는 단일 튜브 시료 준비 방법을 개발하였다. 아민 기능화 된 규조토와 HI의 복합체가 인수공통 병원균인 *Brucella ovis*으로부터의 핵산 추출에 사용되었다. 단일 튜브 접근 방식을 사용하면 20분 내로 튜브 내의 1 집락 형성 단위 (Colony forming unit, CFU)의 수준까지의 병원균의 핵산을 추출할 수 있다. 이 단일 튜브 방식은 핵산과 규토 기질 사이의 가역적인 교차 결합 반응 (reversible cross-linking reaction)을 기반으로 작용한다. 활발한 공유 결합의 형성은 핵산, 특히 RNA를 리보핵산 가수분해 효소 (ribonuclease, RNase)가 풍부한 시료로부터 보호하여 핵산의 세척과 분리 단계의 어려움을 해결해 준다. 이 방법의 성능은 상업용 키트 (10^2-10^3 CFU mL^{-1})보다 10-100 배 우수하지만, 대형 원심 분리기 등의 복잡한 장비가 필요하지 않다. 일반적인 SPE 키트에 비해 단일 튜브 시스템은 인간의 소변과 혈청에서 병원균의 핵산을 효율적으로 분리할 수 있으며 검출 한계가 최대 100 배까지 향상된다 (소변, 혈청 내에서 1 CFU mL^{-1}). 이 시스템은 빠르고 민감하기 때문에 현장 진단 검사에서 시료 준비를 위한 유망한 접근법을 제시한다.

Keywords: Point-of-care, Pathogen diagnosis, Reversible cross-linking reaction, Nucleic acid extraction, Homobifunctional imidoester